

Jointly Learned Symbol Detection and Signal Reflection in RIS-Aided Multi-user MIMO Systems

Liuhan Wang, Nir Shlezinger, George C. Alexandropoulos,
Haiyang Zhang, Baoyun Wang, and Yonina C. Eldar

Abstract—Reconfigurable Intelligent Surfaces (RISs) are regarded as a key technology for future wireless communications, enabling programmable radio propagation environments. However, the passive reflecting feature of RISs induces notable challenges on channel estimation, making coherent symbol detection a challenging task. In this paper, we consider the uplink of RIS-aided multi-user Multiple-Input Multiple-Output (MIMO) systems and propose a Machine Learning (ML) approach to jointly design the multi-antenna receiver and configure the RIS reflection coefficients, which does not require explicit full knowledge of the channel input-output relationship. Our approach devises a ML-based receiver, while the configurations of the RIS reflection patterns affecting the underlying propagation channel are treated as hyperparameters. Based on this system design formulation, we propose a Bayesian ML framework for optimizing the RIS hyperparameters, according to which the transmitted pilots are directly used to jointly tune the RIS and the multi-antenna receiver. Our simulation results demonstrate the capability of the proposed approach to provide reliable communications in non-linear channel conditions corrupted by Gaussian noise.

Index terms— Reconfigurable intelligent surfaces, Bayesian machine learning, reflection configuration, multi-user MIMO.

I. INTRODUCTION

Modern communications systems are subject to constantly growing throughput requirements. In order to meet these demands, Base Stations (BSs) are commonly equipped with multiple antennas, and communicate with several users simultaneously to increase the spectral efficiency [1]. One of the main challenges in such multi-user Multiple-Input Multiple-Output (MIMO) systems is symbol detection, namely, the recovery of the multiple symbols transmitted over the uplink channel at the BS. Conventional detection algorithms, such as those based on the Maximum A-posteriori Probability (MAP) rule, which jointly recovers all the symbols simultaneously, become infeasible as the number of symbols grows. Alternative low complexity symbol detection are usually based on separate detection or iterative interference cancellation methods [2], which allow to achieve MAP-approaching performance at complexity which only grows linearly with the number of users. In addition, even when the channel model is linear and known, inaccurate knowledge of the parameters of the

channel, namely, Channel State Information (CSI) uncertainty, can significantly degrade the performance.

An alternative data-driven approach to model-based algorithms uses Machine Learning (ML). Deep Neural Networks (DNNs), which constitute a popular ML approach, have demonstrated an unprecedented empirical success in various applications, including image and speech processing [3]. Recent years have witnessed growing interest in the application of DNNs for Receiver (RX) design; see detailed surveys in [4]–[7]. Unlike model-based reception, which implements a specified detection rule, ML-based RXs learn how to map the channel outputs into the transmitted symbols from training, namely, they operate in a data-driven manner. Multiple ML-aided MIMO reception architectures have been proposed in the literature, including the application of conventional black-box architectures [8], deep unfolded optimization algorithms such as projected gradient descent [9], [10], and approximate message passing [11]. While the aforementioned RXs involve highly parameterized DNNs, which require massive volumes of data for training, the more recent work [12] designed a data-driven RX which learns to implement the soft iterative interference cancellation symbol detection algorithm of [13] from relatively small labeled data sets.

An additional emerging technology for multi-user wireless communication systems is the consideration of Reconfigurable Intelligent Surfaces (RISs) as enablers for controllable signal propagation conditions [14], [15]. This application builds upon the capability of RISs to generate reconfigurable reflection patterns. An RIS deployed in urban settings can facilitate and improve communication between the BS and multiple users by effectively modifying the propagation of information-bearing signals [16]. The RISs enable the communications system as a whole to overcome harsh non Line-Of-Sight (LOS) conditions and improve coverage, when the surface close to the BS or the users, without increasing transmission power. Nonetheless, the fact that RISs are passive devices, which only reflect their impinging signals in a configurable manner, gives rise to a multitude of signal processing challenges, including complex and costly channel estimation [17]. Furthermore, identifying the proper configuration of the RIS reflection patterns is a difficult task and requires accurate knowledge of the underlying channel [18], which in turn is quite challenging to acquire. This motivates the application of model-agnostic data-driven ML for tuning RISs, which is the focus here.

In this paper, considering the uplink of an RIS-empowered multi-user MIMO communication system, we present an ML-based approach to jointly tackle the problem of symbol de-

L. Wang and B. Wang are with the School of Communication and Information Engineering, Nanjing University of Posts and Telecommunications, Nanjing, China (e-mail:2331829836@qq.com; bywang@njupt.edu.cn). N. Shlezinger is with the School of Electrical and Computer Engineering, Ben-Gurion University of the Negev, Beer-Sheva, Israel (e-mail: nirshl@bgu.ac.il). G. C. Alexandropoulos is with the Department of Informatics and Telecommunications, National and Kapodistrian University of Athens, Greece (e-mail: alexandg@di.uoa.gr). H. Zhang and Y. C. Eldar are with the Faculty of Math and Computer Science, Weizmann Institute of Science, Rehovot, Israel (e-mail: {haiyang.zhang; yonina}@weizmann.ac.il). This work has been partially supported by the EU H2020 RISE-6G project under grant number 101017011.

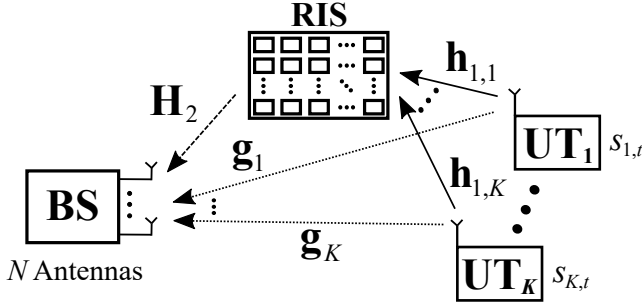


Fig. 1. The considered RIS-empowered multi-user MIMO communication system operating in the uplink direction.

tection at the BS's multi-antenna RX, along with the configuration of the RIS reflection coefficients. We adopt the recent DeepSIC reception of [12] at the BS and treat the RIS phase configuration as hyperparameters of the learning procedure. We devise an algorithm based on Bayesian Optimization (BO) for the RIS configuration, which alternatively combined with the DNN-aided RX to enable joint optimization of the RIS and the RX with small amounts for pilot signals. Our numerical results demonstrate the efficacy of the proposed model-agnostic DNN-based learning approach for providing reliable RIS-empowered multi-user MIMO communications, without relying on channel modeling and CSI estimation.

The rest of this paper is organized as follows. Section II includes the system model and problem formulation, while Section III details the proposed learning approach for jointly learning the multi-antenna RX and the RIS phase configuration. Section IV presents the simulation results, and the paper's conclusions are drawn in Section V. Throughout the paper, we use low-case letters for scalars (e.g. x), lower case bold-faced letters for vectors (e.g., \mathbf{x}), upper case bold-faced letters for matrices (e.g., \mathbf{X}), and calligraphic letters for sets (e.g., \mathcal{X}). The i -th element of \mathbf{x} is denoted by $[\mathbf{x}]_i$, $\mathbb{E}[\cdot]$ is the expectation operator, and $(\cdot)^T$ returns the transpose.

II. SYSTEM MODEL AND DESIGN OBJECTIVE

A. System Model

We focus on the uplink of cellular networks and consider a single-cell including a BS with N antenna elements that serves K User Terminals (UTs), as illustrated in Fig. 1. This uplink communication is assumed to be assisted by an RIS with P unit elements [18]. An RIS controller, which is accessible by the BS, handles the metasurface's reflection configuration [19]. We assume that the BS makes use of the DNN-based RX in [12], which particularly implements a data-driven detector. In order to train the BS, in each time instance t , the UTs transmit known pilot symbols, denoted $\mathbf{s}_t \triangleq [s_{1,t} s_{2,t} \cdots s_{K,t}] \in \mathcal{S}^{K \times 1}$, where \mathcal{S} is a discrete constellation set of size M .

We assume that the input-output relationship of the wireless channel is given by some stochastic transformation parameterized by the RIS phase configuration vector $\phi \in \mathcal{C}^P$. Considering finite resolution phase shifting values for the RIS unit elements, each n -th element (with $n = 1, 2, \dots, P$) of ϕ can be modeled as follows [20]:

$$[\phi]_n \in \left\{ e^{j2^{1-b}\pi m} \right\}_{m=0}^{2^b-1}, \quad (1)$$

where b is the phase resolution in number of bits; clearly, the different number of phase shifting values per RIS unit element is 2^b . Based on the latter expression, we represent the feasible set of RIS phase configuration vectors as Θ , i.e., $\phi \in \Theta \subset \mathcal{C}^{P \times 1}$. The channel output, i.e., the baseband received at the N BS antenna elements, at the time instance t is modeled as

$$\mathbf{y}_t = f_\phi(\mathbf{s}_t) \in \mathcal{C}^N, \quad (2)$$

where $f_\phi(\cdot)$ represents an unknown generic function that depends on ϕ . For the special case of the conventional linear Gaussian channels, this function takes the following form [14]:

$$f_\phi^{(G)}(\mathbf{s}_t) \triangleq (\mathbf{H}_2 \Phi \mathbf{H}_1 + \mathbf{G}) \mathbf{s}_t + \mathbf{n}_t, \quad (3)$$

where $\Phi \triangleq \text{diag}(\phi)$, $\mathbf{H}_1 \triangleq [\mathbf{h}_{1,1} \mathbf{h}_{1,2} \cdots \mathbf{h}_{1,K}] \in \mathcal{C}^{P \times K}$ denotes the wireless channel gain matrix between the RIS unit elements and the UTs ($\mathbf{h}_{1,k} \in \mathcal{C}^{P \times 1}$ with $k = 1, 2, \dots, K$ represents the channel for the k -th UT), $\mathbf{H}_2 \in \mathcal{C}^{N \times P}$ represents the channel between the BS and RIS, and $\mathbf{G} \triangleq [\mathbf{g}_1 \mathbf{g}_2 \cdots \mathbf{g}_K] \in \mathcal{C}^{N \times K}$ is the direct channel matrix between the BS and the UTs ($\mathbf{g}_k \in \mathcal{C}^{N \times 1}$ represents the channel for the k -th UT). In addition, $\mathbf{n}_t \in \mathcal{C}^N$ is the Additive White Gaussian Noise (AWGN) vector, which is usually modeled as having zero-mean elements and covariance matrix $\sigma^2 \mathbf{I}_N$.

B. Problem Formulation

The BS uses the baseband received signal vector \mathbf{y}_t , i.e., the channel output in (2), along with the prior knowledge of the pilot symbols \mathbf{s}_t , to train its DNN-based detector (i.e., multi-antenna RX) and decide the RIS phase configuration vector ϕ . Consequently, by letting $\theta \in \mathcal{C}^{M \times 1}$ denote the weights of the BS's DNN-based symbol detector, our goal is to jointly design θ and ϕ to minimize the Bit Error Rate (BER). By representing the DNN operation as the mapping $\psi_\theta(\cdot) : \mathcal{C}^{N \times 1} \rightarrow \mathcal{S}^{K \times 1}$, we seek to minimize the following objective function:

$$\mathcal{F}(\theta; \phi) = \mathbb{E} \left\{ \|\mathbf{s}_t - \psi_\theta(f_\phi(\mathbf{s}_t))\|_0 \right\}. \quad (4)$$

Obviously, this objective approaches its minimal value of 0 when the DNN operation mimics the inverse function of $f_\phi(\cdot)$. The BER captures the performance of the considered communication system, which is actually determined by the DNN-based RX and the RIS phase configuration, i.e., θ and ϕ . For the DNN design, we need periodic pilots to optimize θ and ϕ to gradually improve the system performance.

III. JOINT MULTI-USER RX AND RIS DESIGN

In this section, we first present our approach for optimizing the considered design objective, and then describe the DNN-based RX structure together with the adopted training scheme. We also present our method for jointly optimizing the DNN-based multi-antenna RX and the RIS phase configuration.

A. Proposed Optimization Approach

We seek to jointly adapt the parameters of the proposed DNN-based RX, parameterized by θ , along with the RIS phase configuration vector ϕ , without explicit knowledge of the channel input-output relationship. The lack of such CSI renders conventional ML optimization algorithms, e.g., based

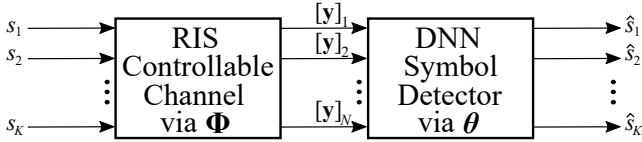


Fig. 2. The phase configurations of the RIS unit elements considered as hyperparameters in the proposed ML-based approach for the joint design of the BS’s multi-antenna RX and the RIS; \hat{s}_k is the estimate for s_k .

on gradient methods and backpropagation [21], [22], infeasible. To tackle this challenge, we note that the RIS parameters effectively modify the channel conditions, and can thus be considered as *hyperparameters*. Those parameters affect the learning process, but are not directly learned in it, i.e., by the DNN-based symbol detector, as illustrated in Fig. 2. This formulation accounts for the fact that the overall task of the system is to recover the transmitted symbols, which is carried out using the DNN-based detector. Modeling the elements of ϕ as hyperparameters motivates the application of BO for tuning them along with the detector [23].

Conventional ML parameters, e.g., the weights of a neural network which control its mapping, are learned during the training process. Hyperparameters are parameters of ML algorithms that control the model’s class, e.g., the network architecture [24], or the learning process, e.g., the learning rate [25] and the optimization rule [26]. They can be either chosen from a discrete set or from a continuous range, and the space which the hyperparameters are chosen from is referred to, henceforth, as the *search space*. The main difference between learning the parameters of an ML model and optimizing its hyperparameters follows from the fact that: while one can commonly compute the gradient of a model’s loss function with respect to its parameters, evaluating the gradients with respect to the hyperparameters is often infeasible. Consequently, gradient-based methods, which are the leading workhorse in training DNN parameters [27, Ch. 6], are often not applicable.

It is evident from (4) that the expected BER in the objective function $\mathcal{F}(\theta; \phi)$ cannot be computed without prior knowledge of the underlying statistical model, and as such, it must be approximated using its empirical form. This requires the transmission of T pilot symbols, i.e., a labeled set of the form $\{\mathbf{s}_t, \mathbf{y}_t\}_{t=1}^T$ in which \mathbf{y}_t is a realization of $f_\phi(\mathbf{s}_t)$. Furthermore, to facilitate the optimization of the DNN as a set of classifiers, we consider that the output of the DNN-based RX models an estimate of the conditional distribution of each of the transmitted symbols, i.e., $\psi_\theta(\cdot)$ comprises of K vectors of size M , each representing an estimate of the conditional probability of a single symbol. In this case, the ℓ_0 -norm in (4) can be replaced with the cross-entropy loss function. By letting $\psi_\theta(\cdot, \alpha)_k$ represent the estimated probability mass function of the k -th symbol evaluated at realization $\alpha \in \mathcal{S}$, the resulting empirical cross-entropy loss is given by:

$$F(\theta; \phi) = \sum_{t=1}^T \sum_{k=1}^K -\log \psi_\theta(\mathbf{y}_t, [\mathbf{s}_t]_k)_k. \quad (5)$$

Using the latter formulation of the empirical error, one can apply the following two-stage iterative procedure for the

parameters of the BS’s DNN-based RX and those of the RIS phase configuration at each iteration index i :

$$\theta_{i+1} = \arg \min_{\theta} F(\theta; \phi_i), \quad (6)$$

$$\phi_{i+1} = \arg \min_{\phi} F(\theta_{i+1}; \phi). \quad (7)$$

We note that, at each iteration i in the above approach, the transmission of additional T pilots is required. Recall that, at each time ϕ is modified, a channel input-output function $f_\phi(\cdot)$ is generated, and a new training set $\{\mathbf{s}_t, \mathbf{y}_t\}_{t=1}^T$ is required. Furthermore, while the optimization of the DNN parameters θ in (6) can be carried out using conventional gradient-based methods, updating ϕ in (7) involves complex optimization with an objective function which is expensive to compute. This follows due to the fact that the hyperparameters ϕ affect the channel mapping $f_\phi(\cdot)$, hence, the parameterization of $f_\phi(\cdot)$ is not explicit, i.e., it is not a known DNN architecture as the symbol detector is, and thus the RX has no direct access to it. This indicates that the usage of Bayesian hyperparameter optimization techniques [28] for updating ϕ should be suitable for the problem at hand, and can be simple to apply using existing BO toolboxes, e.g., [29]. Therefore, the optimization of the objective actually accounts for the optimization of two parameters, i.e., θ and ϕ .

B. Multi-User Receiver Model

We adopt the DeepSIC RX [12], which is a DNN-based soft RX implementing the traditional iterative interference cancellation method, based on channel modeling by means of deep learning, and expands to channel-model-independent implementations.

1) *Receiver Architecture*: The RX uses an iterative fashion to achieve interference cancellation. To this end, the symbols transmitted by other UTs are regarded as interference symbols for the k -th UT. The detector operates iteratively: in every iteration $q \in \{1, 2, \dots, Q\} \triangleq \mathcal{Q}$, an estimate of the conditional distribution, denoted by $\mathbf{p}_k^{(q)}$, of \mathbf{s}_k for a given channel output \mathbf{y} is generated for each UT $k \in \mathcal{K} \triangleq \{1, 2, \dots, K\}$ using the corresponding estimate of the interference symbols $\{\mathbf{s}_l\}_{l \neq k}$ obtained in the previous iteration. Here, we denote \mathbf{s}_k as the symbols transmitted by the k -th UT at each time instance. The purpose of interference cancellation is achieved through continuous iteration, and the outputs of the DNN at the last iteration are used for decoding in a hard decision manner. The whole process is illustrated in the Fig. 3(a). The DNN of each UT in the entire structure can be viewed as a building block and its output is the conditional probability of each UT’s symbols. Therefore, it can be seen as a classifier that is agnostic of the channel model. The output for the k -th building block of q -th iteration is $\hat{\mathbf{p}}_k^{(q)}$, which is the estimated conditional probability of \mathbf{s}_k given \mathbf{y} based on $\{\hat{\mathbf{p}}_l^{(q-1)}\}_{l \neq k}$.

The structure for the DNN for each UT’s symbol is shown in Fig. 3(b). Each soft estimate is produced using a multi-layer fully connected structure with softmax output layer. For simplicity, we illustrate the DNN architecture with real-valued channels, as the considered channel model with complex values can be represented by real vectors of an extended dimension. Since we use classification DNNs for

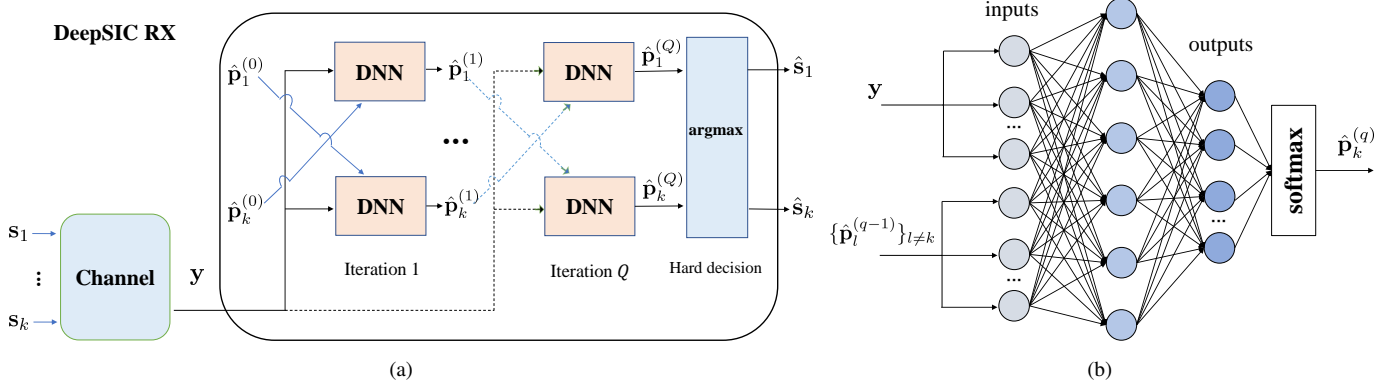


Fig. 3. Structure of the overall DNN-based multi-user RX. (a) DeepSIC-RX illustration; (b) Detailed structure of each DNN in (a).

soft-estimates, the number of neurons at their output layers depends on the size M of the constellation set. The inputs of each DNN includes the inputs at the BS's N receive antennas, and the conditional probabilities $\{\hat{\mathbf{p}}_l^{(q-1)}\}_{l \neq k}$ of the interfering symbols from the previous iteration. Thus, the number of input neurons is $N + (K-1)(M-1)$. Finally, the initial conditional probabilities for each UT are set to the uniform distribution, i.e., $\{\hat{\mathbf{p}}_k^{(0)}\}_{k=1}^K = M^{-1}$.

2) *Receiver Training*: In order to make the RX realize reliable symbol detection, each DNN needs to be properly trained. We use the data set of N_{tr} pairs of channel inputs and corresponding outputs $\{\tilde{\mathbf{s}}_j, \tilde{\mathbf{y}}_j\}_{j=1}^{N_{\text{tr}}}$ to train the RX in a sequential training fashion. Note that the DNN building blocks do not depend on the iteration index value, and the input of each DNN depends on the channel output \mathbf{y} and the output $\{\hat{\mathbf{p}}_l^{(q-1)}\}_{l \neq k}$ of the trained DNN in the previous iteration. This indicates that the DNNs can be trained separately in a sequential manner to minimize the cross-entropy loss. As such, we can train each DNN with a small number of samples. By letting $\theta_k^{(q)}$ represent the parameters of the k -th DNN at iteration q and writing $\hat{\mathbf{p}}_k^{(q)}(\mathbf{y}, \{\hat{\mathbf{p}}_l^{(q-1)}\}_{l \neq k}, \alpha; \theta_k^{(q)})$ as the entry of $\hat{\mathbf{p}}_k^{(q)}$ corresponding to $\alpha \in \mathcal{S}$, when the parameters and inputs of DNN are $\theta_k^{(q)}$ and $(\mathbf{y}, \{\hat{\mathbf{p}}_l^{(q-1)}\}_{l \neq k})$, respectively, we can re-express the empirical cross-entropy loss in (6) as:

$$\mathcal{L}(\theta_k^{(q)}) = \frac{1}{N_{\text{tr}}} \sum_{j=1}^{N_{\text{tr}}} -\log \hat{\mathbf{p}}_k^{(q)}(\tilde{\mathbf{y}}_j, \{\hat{\mathbf{p}}_{j,l}^{(q-1)}\}_{l \neq k}, (\tilde{\mathbf{s}}_j)_k; \theta_k^{(q)}), \quad (8)$$

where $\{\hat{\mathbf{p}}_{j,l}^{(q-1)}\}_{l \neq k}$ represents the estimated conditional probabilities at the previous iteration associated with $\tilde{\mathbf{y}}_j$. The sequential training method from [12] is summarized in Algorithm 1.

C. Proposed Joint RX and RIS Learning Method

In this section, we first discuss the application of the BO framework to our RIS-empowered multi-user MIMO system design objective, and then present a method to jointly optimize the DNN-based multi-antenna RX and the RIS phase configuration.

1) *RIS Configuration via Bayesian Optimization*: Let $g(\cdot)$ represent the mapping between the reflection coefficients of the RIS and the RX output, and ee focus on finding

Algorithm 1: Sequential Training for the DeepSIC RX

Input : Training data set $\{\tilde{\mathbf{s}}_j, \tilde{\mathbf{y}}_j\}_{j=1}^{N_{\text{tr}}}$, Q , and \mathcal{K} .

Output: Trained DNN parameters $\theta = \{\theta_k^{(q)}\}_{k,q=1}^{K,Q}$.

- 1 **Initialization**: Set $q = 1$, $\{\hat{\mathbf{p}}_k^{(0)}\}_{k=1}^K = M^{-1}$ and $\hat{\mathbf{p}}_{j,k}^{(0)} = \hat{\mathbf{p}}_k^{(0)}$ for every $k \in \mathcal{K}$, and $j \in \{1, 2, \dots, N_{\text{tr}}\}$.
 - 2 **while** $q \leq Q$ **do**
 - 3 **for** $k \in \mathcal{K}$ **do**
 - 4 Set the DNN parameters to $\theta_k^{(q)}$.
 - 5 Train the DNN to minimize (8).
 - 6 Feed $\{\tilde{\mathbf{y}}_j, \{\hat{\mathbf{p}}_{j,l}^{(q-1)}\}_{l \neq k}\}_{j=1}^{N_{\text{tr}}}$ to the trained DNN to obtain $\{\hat{\mathbf{p}}_{j,k}^{(q)}\}_{j=1}^{N_{\text{tr}}}$.
 - 7 Set $q = q + 1$.
 - 8 **end**
 - 9 **end**
-

$\phi^* \triangleq \arg \max_{\phi} g(\phi)$ (or equivalently, one can solve for $\arg \min_{\phi} -g(\phi)$). Since it's hard to acquire knowledge for $g(\cdot)$ (i.e., it's a black box function), traditional gradient methods cannot be applied for learning it. For such cases, the BO formulation can be used which consists, in general, of the following two components: *i*) a *surrogate model* (the most commonly used is the Gaussian Process (GP)) to incorporate prior beliefs about the objective function; and *ii*) an *acquisition function* that directs sampling to areas where an improvement over the current best observation is likely.

Let ϕ_i denote the i -th sample RIS phase configuration and $g(\phi_i)$ the output observation at the RX of the unknown objective function at the point ϕ_i . We also use the set notation $\mathcal{D}_{1:n} \triangleq \{\phi_{1:n}, \mathbf{g}_{1:n}\}$ to represent the observed data pairs; the subscript is used to denote sequences of data, i.e., $\phi_{1:n} \triangleq [\phi_1, \phi_2, \dots, \phi_n]$ and $\mathbf{g}_{1:n} \triangleq [g(\phi_1), g(\phi_2), \dots, g(\phi_n)]$. Following the Bayesian framework, the observation $\mathbf{g}_{1:n}$ can be considered to be drawn randomly from some prior probability distribution. Usually, GP considers the multivariate normal as the prior distribution, having as unknown parameters its n -element mean value vector $\boldsymbol{\mu}$ and its $n \times n$ covariance matrix \mathbf{K} ; the latter is also referred as *kernel* denoted k . A popular choice of the kernel is squared exponential function,

$$k(\phi_i, \phi_j) = \exp\left(-\frac{1}{2} \|\phi_i - \phi_j\|^2\right) \quad (9)$$

Hence, the prior distribution on $\mathbf{g}_{1:n}$ is mathematically expressed as:

$$\mathbf{g}_{1:n} \sim \mathcal{N}(\boldsymbol{\mu}(\phi_{1:n}), \mathbf{K}(\phi_{1:n})), \quad (10)$$

where $\boldsymbol{\mu}(\phi_{1:n})$ and $\mathbf{K}(\phi_{1:n})$ include the sample mean values and the covariance matrix for the observation $\phi_{1:n}$; for simplicity, we will henceforth omit the dependence of these parameters on $\phi_{1:n}$, although implied, and write $\boldsymbol{\mu}_{1:n}$ and $\mathbf{K}_{1:n}$. The latter implies that the observation set $\mathcal{D}_{1:n}$ is used to compute $\mathbf{g}_{1:n}$, thus providing an estimate for the unknown mapping $g(\cdot)$. The BO framework can be then used to predict the next value g_{n+1} at an arbitrary point ϕ_{n+1} , hence refining $g(\cdot)$ estimation. According to the properties of GPs, $\mathbf{g}_{1:n}$ and g_{n+1} (which denotes a new observation at the RX output as a response to a new RIS configuration ϕ_{n+1}) follow the bivariate Gaussian distribution. By using the notation $\tilde{\mathbf{K}}_{1:n,n+1}$ to denote the covariance matrix of that distribution and applying the Bayes' rule, the prediction for the conditional distribution of g_{n+1} , given the observations $\mathcal{D}_{1:n}$ and the RIS phase configuration ϕ_{n+1} , is expressed as:

$$g_{n+1} | \mathcal{D}_{1:n}, \phi_{n+1} \sim \mathcal{N}(\mu_n(\phi_{n+1}), \sigma_n^2(\phi_{n+1})), \quad (11)$$

where the mean and variance are respectively given by:

$$\begin{aligned} \mu_n(\phi_{n+1}) &\triangleq \tilde{\mathbf{K}}_{1:n,n+1}^T \mathbf{K}^{-1}(\mathbf{g}_{1:n} - \boldsymbol{\mu}_{1:n}) + \mu(\phi_{n+1}), \\ \sigma_n^2(\phi_{n+1}) &\triangleq k(\phi_{n+1}, \phi_{n+1}) - \tilde{\mathbf{K}}_{1:n,n+1}^T \mathbf{K}^{-1} \tilde{\mathbf{K}}_{1:n,n+1}. \end{aligned} \quad (12)$$

The latter conditional distribution is called the *posterior* probability distribution. Its mean implies the actual prediction and its variance represents the value of uncertainty. The previous process constitutes the first part of the BO framework. It is a sequential iterative process of obtaining the posterior from the prior and constantly updating the prior. In other words, after modeling the unknown mapping $g(\cdot)$ with GP, we can learn its posterior distribution at any sampling point ϕ_i , which helps us to find its optimal value. When a new observation is collected, we add it to the existing data set to form an enlarged new set, and then, update the prior. Thus, by expanding the observation set, i.e., as n increases for $\mathcal{D}_{1:n}$, the fitted function will approximate the unknown mapping.

The problem now is how to choose the next sampling point efficiently, so that we can find the optimal value with the least number of iterations. This problem can be solved by the second component of BO, i.e., the *acquisition function* which helps to guide the search. In general, every next sample in BO is obtained by maximizing the acquisition function. That is, we want to sample g at $\arg \max_{\phi} p(\phi | \mathcal{D})$, where $p(\cdot)$ represents the generic function of the acquisition function. In this paper, we deploy the popular analytic acquisition function of the Expected Improvement (EI) to find the next sample point for the Bayes' rule. The definition of improvement denoted I for an input ϕ is:

$$I(\phi) \triangleq \max(g_{n+1}(\phi) - g(\phi^+), 0), \quad (13)$$

where $g(\phi^+)$ denotes the currently observed best value and $g_{n+1}(\phi)$ is the mapping output at the next sample point. This function is intuitively easy to understand: it is positive when the prediction is greater than the best observation so far; on

the contrary, it is set to zero. Therefore, the second step in (7) of our iterative procedure can be determined by optimizing the EI acquisition function, i.e.:

$$\phi_{i+1} = \arg \max_{\phi} \mathbb{E}\{\max(g_{n+1}(\phi) - g(\phi^+), 0) | \mathcal{D}_{1:n}\}. \quad (14)$$

It is noted that this function can be evaluated analytically under the GP model [30]. This means that the gradients are available and we can easily optimize this function using relevant toolboxes [27].

2) *Joint RX and RIS Optimization*: As shown in (6) and (7), the proposed joint design approach includes the following sequential iterative procedure: the DNN-based multi-antenna RX is first optimized for multi-user decoding for a given RIS configuration, and then, the RIS optimization is performed via BO to further reduce the BER performance. We consider sending T pilot symbols at each iteration index t and for a given RIS phase configuration to train the DeepSIC RX, with the intention to optimize the parameters θ . When the RIS is optimized and ϕ_{t+1} for the next iteration is obtained, the wireless propagation channel changes. This means that the new RIS configuration ϕ_{t+1} will generate a new function $f_{\phi_{t+1}}(\cdot)$ for the input-output relationship of the wireless channel. Consequently, we need to resend pilots to estimate this channel and retrain the DeepSIC RX for multi-user symbol detection. It is noted that the entire optimization process needs to be carried out alternately in a sequential manner. The steps of the proposed approach are included in Algorithm 2.

In the proposed algorithm, we use the set $\{\mathbf{s}_t, \mathbf{y}_t\}$ to present the channel input and corresponding output at the iteration index t . The set $\mathcal{D}_{1:t}$ includes the data $\{\phi_{1:t}, \text{BER}_{1:t}\}$, with $\text{BER}_{1:t}$ representing the BER performances of the trained DeepSIC RX up to the time index t , which is used for the proposed BO method. The RX training in Step 5 is implemented with Algorithm 1. We also use additional UT data to validate the trained RX, by computing the BER. At the end of the algorithmic iterations N_{bo} , we select the RIS phase configuration corresponding to the minimum BER, i.e., ϕ^* , as shown in Step 10. It is worth noting that after obtaining the optimal ϕ^* , we still choose to transmit pilots, in particular the \mathbf{s}_1 sent during the first iteration, to form the corresponding channel output \mathbf{y}^* for retraining the DeepSIC RX. In this way, the best parameters of the trained DNN and the RIS, i.e., θ^* and ϕ^* , are obtained. It is noted that the first algorithmic iteration is considered as the initial reference and the remaining $N_{\text{bo}} - 1$ iterations are used for the optimization process. At the end of the process, we re-send \mathbf{s}_1 to verify whether the RIS parameters have been optimized. In addition, at each iteration index t , the T transmitted pilots are chosen to be different in order to improve the generalization capability of the system. Also, the initial RIS configuration ϕ_1 is randomly chosen since there is no CSI available at the system.

D. Discussion

The proposed joint RX and RIS design approach is quite flexible. During the BO process, we model the mapping between the RIS and RX, which is independent of the specific RX structure, i.e., the RX is relatively independent. This

Algorithm 2: ML-Based Joint RX and RIS Design

- 1 **Initialization:** Generate the RIS phase configuration ϕ_1 and the DNN parameters θ_1 , and initialize the observation set as $\mathcal{D}_{1:1} = \{\emptyset\}$.
 - 2 **for** $t = 1, 2, \dots, N_{\text{bo}}$ **do**
 - 3 The UTs make use of the T pilots \mathbf{s}_t and the BS sets as θ_t the parameters of its DNN-based RX.
 - 4 The RIS realizes ϕ_t and the data set $(\mathbf{s}_t, \mathbf{y}_t)$ is generated at the RX input after UTs' transmission.
 - 5 The RX is trained to obtain θ_{t+1} and BER_t .
 - 6 The new data set (ϕ_t, BER_t) is generated and appended to the existing set $\mathcal{D}_{1:t-1}$.
 - 7 The data set $\mathcal{D}_{1:t} = \{\phi_{1:t}, \text{BER}_{1:t}\}$ is formulated to estimate $g(\cdot)$ via the BO approach.
 - 8 Solve (14) to get the next sample ϕ_{t+1} .
 - 9 **end**
 - 10 Set $\phi^* = \phi_{t^*}$ where $t^* = \arg \min_t \text{BER}_{1:N_{\text{bo}}}$.
 - 11 Run Steps 3–5 with \mathbf{s}_1 and ϕ^* to obtain θ^* for the RX.
 - 12 **Output:** The joint design ϕ^* and θ^* .
-

greatly improves the scalability of the framework. The deployed DeepSIC RX [12] is suitable for multi-user MIMO scenarios, implementing a model-based ML algorithm, but also extending it to a channel-model-independent realizations; this is suitable for both linear and non-linear channels. Each DNN building block in DeepSIC is trained separately, thus, its complexity increases linearly with the DeepSIC of UTs; this is very beneficial for MIMO systems. In addition, DeepSIC allows to complete the training process with a small number of training sets, i.e., we can send few pilots for training at each iteration. The computational complexity of the BO approach to optimize the RIS is acceptable. Since we consider probabilistic modeling, the problem of optimizing a black box function is transformed into that of optimizing an acquisition function, which has reduced computational complexity.

The training of the DeepSIC RX is carried out in an iterative way, which means that the improvement in the BER performance is at the cost of increasing training time. Note that in Algorithm 2, the DeepSIC RX needs to be retrained at each iteration. This happens because we need to continuously obtain the data used to fit the target mapping in the BO formulation, and the system performance can be gradually improved as the amount of data increases. Therefore, the BER improvement in the proposed two-stage iteration is at the cost of increasing time complexity. Actually, the BO method is typically applied to adapt a limited amount of parameters. One can extend it to high dimensions [31]; we leave this for a future extension.

IV. NUMERICAL RESULTS

A. Simulation Parameters

The scenario we consider is the uplink of a MIMO communication system assisted by an RIS. There exist $K = 5$ UTs in the system, the BS has $N = 5$ antenna elements, and the RIS consists of $P = 18$. The considered channel model follows (3), where the channel matrices \mathbf{H}_1 and \mathbf{G} follow the Rayleigh distribution, while \mathbf{H}_2 is a Rician channel. As such, we have modeled each column of \mathbf{H}_1 and \mathbf{G} as $\mathbf{h}_{1,k} = \gamma \tilde{\mathbf{h}}_{1,k}$ and $\mathbf{g}_k = \gamma \tilde{\mathbf{g}}_k$, respectively, where γ is the passloss factor and

$\tilde{\mathbf{h}}_{1,k}, \gamma \tilde{\mathbf{g}}_k \sim \mathcal{CN}(0, \mathbf{I}_P)$. The channel matrix \mathbf{H}_2 was modeled as follows:

$$\mathbf{H}_2 = \beta \left(\sqrt{\frac{\kappa}{1+\kappa}} \tilde{\mathbf{H}}_2^{\text{LOS}} + \sqrt{\frac{1}{1+\kappa}} \tilde{\mathbf{H}}_2^{\text{NLOS}} \right), \quad (15)$$

where β and κ denote the pathloss and Rician factors, respectively. The superscripts 'LOS' and 'NLOS' represent the LOS and non-LOS components of the channel. These channel components in the previous expression were both modeled as standard Gaussian channel matrices. In the simulations, we have set the passloss factors β and γ to be normalized to 1, and the Rician factor κ was set 10.

The DNN structure of the DeepSIC RX was chosen to have three fully-connected layers: the $N + (K - 1)(M - 1) \times 60$ first layer followed by sigmoid activation, the 60×30 second layer followed by ReLU activation, and the $30 \times M$ third layer. The transmitted symbols were randomly generated from the QPSK constellation, i.e., $\mathcal{S}_{\text{qpsk}} = \{1 + j, -1 + j, -1 - j, 1 - j\}$. Note that this modulation scheme can be represented equivalently by the BPSK constellation, i.e., $\mathcal{S}_{\text{bpsk}} = \{-1, 1\}$ in the following sense: a 5×5 complex channel with QPSK signaling is actually equivalent to a 10×10 real channel with BPSK signaling. This transformation can be actually used to simplify simulations. Since the input data \mathbf{y} at the DNN-based RX cannot be complex, we have given as inputs the real and imaginary parts of this vector. The number of iterations Q for each DNN run was set to 5 in Algorithm 1 and the optimizer used was the ADAM with learning rate 0.01. We have used Python as the simulation environment and we realized BO via Botorch based on Pytorch, which is a BO toolbox.

B. BER Performance Results

We first evaluated the BER performance versus the signal-to-noise ratio (SNR), defined as $1/\sigma^2$, for a fixed RIS configuration in order to solely optimize the DeepSIC RX and verify its performance. Then, we evaluated the BER with the proposed joint DeepSIC RX and RIS optimization, which is described by the two-stage iteration method summarized in Algorithm 2. The results in Fig. 4(a) were obtained with a training set of 1000 samples and a testing data with more than 80000 symbols. The total number of iterations for the BO part were set as $N_{\text{bo}} = 25$. It can be seen that when RIS is fixed, the DeepSIC RX can achieve a good BER performance with a small training data set, and as expected, BER decreases gradually with the SNR. Interestingly, when we also optimize the RIS phase configurations, the BER gets further reduced. For example, for both cases to achieve the BER value 10^{-3} , there will be more than 2 dB gain after optimizing the RIS.

In Fig. 4(b), we evaluate the BER versus the BO iteration number N_{bo} for the fixed SNR value -8 dB. It can be concluded that the BER decreases with increasing N_{bo} . Note that in Algorithm 2, we get the next sample by optimizing the acquisition function. In this subfigure, we also simulated the case where the next sample point (i.e., next RIS configuration) was generated in a random way. Namely, other conditions remained unchanged and we transmitted the same pilots at each iteration, while randomly generating the RIS phase configurations. This random generation yields a straight BER

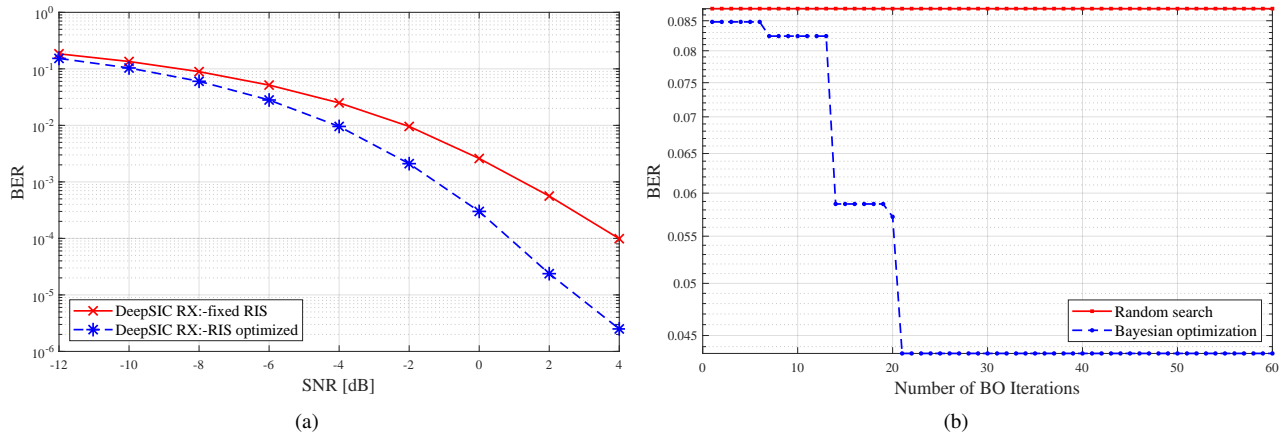


Fig. 4. The BER performance of the proposed ML-based joint RX and RIS optimization: (a) versus the SNR in dB; (b): versus the iteration number N_{bo} .

curve, which means that none of the chosen RIS configurations improved the BER in the considered 60 iterations. Recall that, at each iteration in our proposed approach, we need to send pilot signals and train the DeepSIC RX receiver whenever the RIS configuration changes. This results in training overhead, implying that the RIS configuration search needs to perform efficiently, improving the BER sequentially. As shown, our BO method is more stable than the random selection strategy, yielding better RIS configurations (in terms of BER) with fewer algorithmic iterations.

V. CONCLUSIONS

In this paper, we proposed a joint optimization approach for reception and RIS phase configuration targeting reliable symbol detection in the uplink of RIS-aided multi-user MIMO communication systems. We considered a DNN-based RX which was combined with BO in a two-stage alternating optimization algorithm, requiring periodical transmissions of small numbers of pilot symbols for convergence. Our BER performance evaluation results demonstrated the efficacy of the proposed model-agnostic DNN-based learning approach.

REFERENCES

- [1] T. L. Marzetta, "Noncooperative cellular wireless with unlimited numbers of base station antennas," *IEEE Trans. Wireless Commun.*, vol. 9, no. 11, p. 3590, Nov. 2010.
- [2] J. G. Andrews, "Interference cancellation for cellular systems: a contemporary overview," *IEEE Wireless Communications*, vol. 12, no. 2, pp. 19–29, 2005.
- [3] Y. LeCun *et al.*, "Deep learning," *Nature*, vol. 521, no. 7553, p. 436, 2015.
- [4] T. O'Shea and J. Hoydis, "An introduction to deep learning for the physical layer," *IEEE Trans. Cogn. Commun. Netw.*, vol. 3, no. 4, pp. 563–575, Dec. 2017.
- [5] Q. Mao *et al.*, "Deep learning for intelligent wireless networks: A comprehensive survey," *IEEE Commun. Surveys Tuts.*, vol. 20, no. 4, pp. 2595–2621, 2018.
- [6] D. Gündüz *et al.*, "Machine learning in the air," *IEEE J. Sel. Areas Commun.*, vol. 37, no. 10, pp. 2184–2199, 2019.
- [7] A. Balatsoukas-Stimming and C. Studer, "Deep unfolding for communications systems: A survey and some new directions," *preprint arXiv:1906.05774*, 2019.
- [8] Y. Liao *et al.*, "Deep neural network symbol detection for millimeter wave communications," *preprint arXiv:1907.11294*, 2019.
- [9] N. Samuel *et al.*, "Learning to detect," *IEEE Trans. Signal Process.*, vol. 67, no. 10, pp. 2554–2564, May 2019.
- [10] S. Khobahi *et al.*, "LoRD-Net: Unfolded deep detection network with low-resolution receivers," *IEEE Trans. Signal Process.*, early access, 2021.
- [11] H. He *et al.*, "A model-driven deep learning network for MIMO detection," in *Proc. IEEE GlobSIP*, 2018.
- [12] N. Shlezinger *et al.*, "DeepSIC: Deep soft interference cancellation for multiuser MIMO detection," *IEEE Trans. Wireless Commun.*, vol. 20, no. 2, pp. 1349–1362, Feb. 2021.
- [13] W.-J. Choi *et al.*, "Iterative soft interference cancellation for multiple antenna systems," in *Proc. IEEE WCNC*, 2000.
- [14] C. Huang *et al.*, "Reconfigurable intelligent surfaces for energy efficiency in wireless communication," *IEEE Trans. Wireless Commun.*, vol. 18, no. 8, pp. 4157–4170, Aug. 2019.
- [15] M. Di Renzo *et al.*, "Smart radio environments empowered by reconfigurable AI meta-surfaces: an idea whose time has come," *EURASIP J. Wireless Commun. Net.*, vol. 2019, no. 1, pp. 1–20, May 2019.
- [16] G. C. Alexandropoulos, G. Lerossey *et al.*, "Reconfigurable intelligent surfaces and metamaterials: The potential of wave propagation control for 6G wireless communications," *IEEE ComSoc TCCN Newsl.*, vol. 6, no. 1, pp. 25–37, Jun. 2020.
- [17] G. C. Alexandropoulos *et al.*, "Hybrid reconfigurable intelligent meta-surfaces: Enabling simultaneous tunable reflections and sensing for 6G wireless communications," *preprint arXiv:2104.04690*, 2021.
- [18] —, "Reconfigurable intelligent surfaces for rich scattering wireless communications: Recent experiments, challenges, and opportunities," *IEEE Commun. Mag.*, vol. 59, no. 6, pp. 28–34, Jun. 2021.
- [19] E. Calvanese Strinati *et al.*, "Reconfigurable, intelligent, and sustainable wireless environments for 6G smart connectivity," *IEEE Commun. Mag.*, to appear, 2021.
- [20] C. Huang *et al.*, "Energy efficient multi-user MISO communication using low resolution large intelligent surfaces," in *Proc. IEEE GLOBE-COM*, Dec. 2018.
- [21] —, "Indoor signal focusing with deep learning designed reconfigurable intelligent surfaces," in *Proc. IEEE SPAWC*, Jul. 2019.
- [22] G. C. Alexandropoulos *et al.*, "Phase configuration learning in wireless networks with multiple reconfigurable intelligent surfaces," in *Proc. IEEE GLOBE-COM*, Dec. 2020.
- [23] T. Yu and H. Zhu, "Hyper-parameter optimization: A review of algorithms and applications," *preprint arXiv:2003.05689*, 2020.
- [24] O. Vinyals *et al.*, "Matching networks for one shot learning," in *Adv. Neural Inf. Process. Sys.*, 2016, pp. 3630–3638.
- [25] D. Maclaurin *et al.*, "Gradient-based hyperparameter optimization through reversible learning," in *IEEE ICML*, 2015.
- [26] O. Wichrowska *et al.*, "Learned optimizers that scale and generalize," in *IEEE ICML*, 2017.
- [27] I. Goodfellow, Y. Bengio, and A. Courville, *Deep learning*. MIT press, 2016.
- [28] E. Brochu *et al.*, "A tutorial on bayesian optimization of expensive cost functions, with application to active user modeling and hierarchical reinforcement learning," *preprint arXiv:1012.2599*, 2010.
- [29] M. Balandat *et al.*, "Botorch: Programmable bayesian optimization in pytorch," *preprint arXiv:1910.06403*, 2019.
- [30] D. R. Jones *et al.*, "Efficient global optimization of expensive black-box functions," *J. Global Opt.*, vol. 13, no. 4, pp. 455–492, 1998.
- [31] E. Han *et al.*, "High-dimensional Bayesian optimization via tree-structured additive models," *preprint arXiv:2012.13088*, 2020.